Output mode characteristics of an in-phase locked gain waveguide array CO_2 laser

Sha Peng-Fei(沙鹏飞), Xin Jian-Guo(辛建国)†, Zhou Ying(周 英), and Liu Zheng-Fan(刘正帆)

School of Optoelectronics, Beijing Institute of Technology, Beijing 100081, *China*

(Received 4 January 2011; revised manuscript received 12 March 2011)

In this paper, experimental and theoretical studies of the output mode characteristics of an in-phase locked gain waveguide array CO_2 laser are reported. The experimental results of the optical oscillation mode frequency, the far-field intensity distribution and the burnt pattern of the sliced waveguide array laser are obtained. A revised mode expression of the rectangle waveguide, which is suited for this waveguide array CO_2 laser, is proposed. The theoretical simulation results based on the revised mode expression are shown to be in good agreement with the experimental results.

Keywords: waveguide array, phase coupling, CO_2 laser

PACS: 42.55.Lt, 42.60.Da, 42.60.Fc **DOI:** 10.1088/1674-1056/20/8/084204

1. Introduction

The phase-locked array laser has been widely studied because it can achieve a high brightness laser output. In the past few decades, in order to obtain in-phase locked output, many techniques and structures have been proposed, especially in the field of semiconductor lasers,[1,2] solid lasers[3,4], and gas lasers.[5−10] Although many papers on CO_2 waveguide array lasers have been published, the mode characteristics and the relative theoretical calculation are rarely reported. In 1984, Butler *et al.*[11] reported the first coupled-mode analysis for an array of N identical elements by using their coupled-mode model, thereby interpreting many published experimental results. However, in those experiments, all the gain regions were a few micrometers.

In this paper, based on Hall's waveguide array laser structure,[12] the sliced waveguide array laser is proposed; the experimental results of the optical oscillation mode frequency, the far-field intensity distribution and the burnt pattern of the sliced waveguide array laser are obtained. To explain the experimental results, a revised mode expression based on the Gaussian mode[13−15] and the normal mode[13] of the rectangle waveguide is proposed, and it is shown that the theoretical simulation results based on the revised mode expression are in good agreement with the experimental results.

†Corresponding author. E-mail: xinjgbit@163.com

© 2011 Chinese Physical Society and IOP Publishing Ltd

2. Theoretical analysis and calculation

According to the coupling formula[11,16,17] of the N-unit array, the intensity distribution $E(x,y)$ is given by

$$E(x,y)=\left[\sum_{n=1}^{N}c_n\varepsilon_n(x,y)\right]\mathrm{e}^{\mathrm{i}\beta z}, \tag{1}$$

where $c_n=\sin(ns\pi/(N+1))(n=1,2,\ldots,N)$ is the coupling coefficient between adjacent waveguides; $\varepsilon_n(x,y)$ is the expression of the intensity distribution for the n-th element of the array laser, in which the mode coupling between the different propagation constants is ignored; β is the propagation constant of the waveguide array coupled mode.

For c_n, s can be any integer value among $[1,N]$, each s corresponds to a value of c_n. Then there are N independent expressions for c_n. The positive or negative value of the corresponding c_n will change with s value. For an in-phase locked laser output, $s=1$. Then $c_n=\sin(n\pi/(N+1))$. So when the laser output is in-phase locked,

$$E(x,y)=\left[\sum_{n=1}^{N}\sin\left(\frac{n\pi}{N+1}\right)\varepsilon_n(x,y)\right]\mathrm{e}^{\mathrm{i}\beta z},\quad (n=1,2,\ldots,N). \tag{2}$$

Because of the independence between x and y,

$$E(x)=\left[\sum_{n=1}^{N}\sin\left(\frac{n\pi}{N+1}\right)\varepsilon_n(x)\right]\mathrm{e}^{\mathrm{i}\beta z}. \tag{3}$$

From Eq. (3), it can be seen that $E(x)$ is determined by the function $\varepsilon(x)$. However, as is known, for the waveguide laser, the optical field propagates in the waveguide in the normal form of a waveguide mode which can be described by the following equation[13]

$$\varepsilon(x) = \cos\left(\frac{\pi}{2a}x\right)\mathrm{rect}(x/a)\,\mathrm{e}^{\mathrm{i}\beta_0 z}, \tag{4}$$

where a and b are the waveguide transverse sizes in the x and the y directions, respectively. The optical field propagates between the resonator mirror and the waveguide end in free space, which should be in the form of Gaussian mode and can be described by the following equation:[13−15]

$$\varepsilon(x) = A\frac{1}{w(z)}\,\mathrm{e}^{-x^2/w^2(z)} \times \exp\left[-\mathrm{i}k\left(z+\frac{x^2}{2R(z)}\right)+\mathrm{i}\,\mathrm{arctg}\left(\frac{z}{f}\right)\right]. \tag{5}$$

The relationship between the beam radius of a Gaussian beam and the waveguide transverse size can be determined by the following equations:[12]

$$w_0 = 0.7032a,\ \text{(square)},$$

$$w_0 = 0.6435a,\ \text{(round)}.$$

The simulations of the above two expressions both have differences from the experimental results, which were obtained with the sliced waveguide array laser. To explain the experimental results, a revised mode expression is proposed, which is based on the above expressions.

Considering the fact that the optical field propagates between the resonator mirror and waveguide end in free space in the form of Gaussian beam, the waveguide aperture will restrain the beam in transverse for the beam to be coupled into the waveguide, the function $\varepsilon(x)$ should be expressed as

$$\varepsilon(x) = A\frac{1}{w(z)}\exp\left(-\frac{x^2}{w^2(z)}\right) \times \exp\left\{-\mathrm{i}k\left(z+\frac{x^2}{2R(z)}\right)+\mathrm{i}\,\mathrm{arctg}\left(\frac{z}{f}\right)\right\} \times\mathrm{rect}\left(\frac{x}{a}\right). \tag{6}$$

We call it an "aperture Gaussian". When there is only one mode frequency oscillation in the waveguide array cavity, the output mode of the N-unit array locked in phase can be written as

$$E(x) = \left\{\sum_{n=1}^{N}\sin\left(\frac{n\pi}{N+1}\right)\exp\left[-\frac{x_n^2}{w^2(z)}\right] \times\exp\left[-\mathrm{i}k\left(z+\frac{x_n^2}{2R(z)}\right)+\mathrm{i}\,\mathrm{arctg}\left(\frac{z}{f}\right)\right] \times\frac{1}{w(z)}\mathrm{rect}\left(\frac{x_n}{a}\right)\right\}\exp(\mathrm{i}\beta z). \tag{7}$$

Based on Eq. (7), the theoretical simulation results are shown in Figs. 1–3.

Figure 1 shows the far-field intensity distribution and the cross section of the output beam when there is only one oscillation mode in the cavity. From Fig. 1(a), it can be seen that the far-field intensity distribution is a spatially suppressed single peak distribution with two negligible side lobes. Figure 1(b) demonstrates the cross section of the output beam, which is a one-dimensional single interference strip and the simulation result of the output beam that is obtained at a free propagation distance of 4.5 m without focusing.

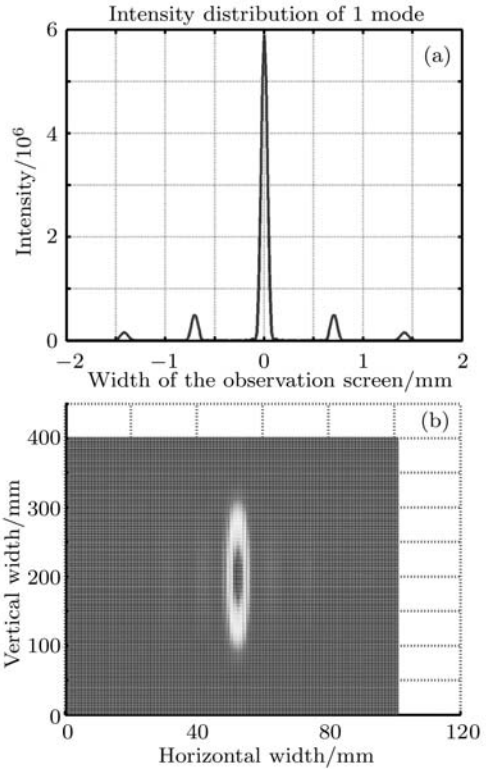


Fig. 1. Theoretical simulation results for one mode oscillation, showing (a) the far-field intensity distribution of the output beam, and (b) the output beam cross section at 4.5 m.

Figure 2 indicates the far-field intensity distribution and the cross section of the output beam when there are two oscillation modes in the cavity. In this situation, the optical field of the waveguide array is coupled into two groups which respectively oscillate at one frequency. Figure 2(a) exhibits that the far-field intensity distribution is a spatially suppressed distribution with two peaks and negligible side lobes; figure 2(b) displays the cross section of the output beam

at 4.5 m which has two one-dimensional interference strips with a central intensity valley.

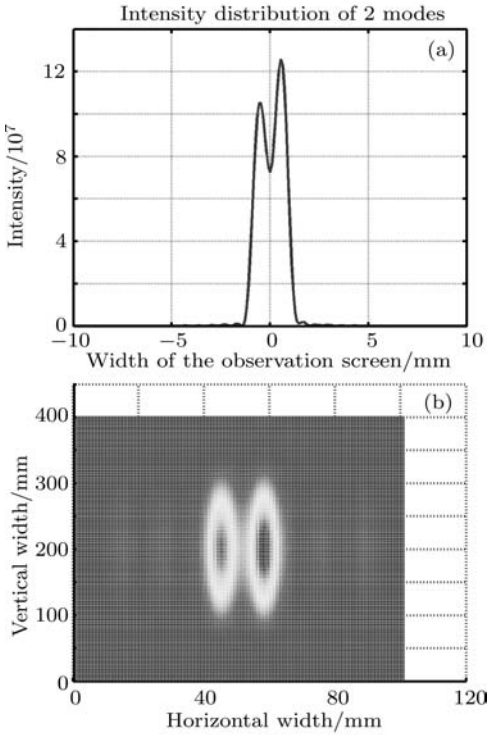


Fig. 2. Theoretical simulation results of two-mode oscillations, showing (a) the far field intensity distribution of the output beam, and (b) the output beam cross section at 4.5 m.

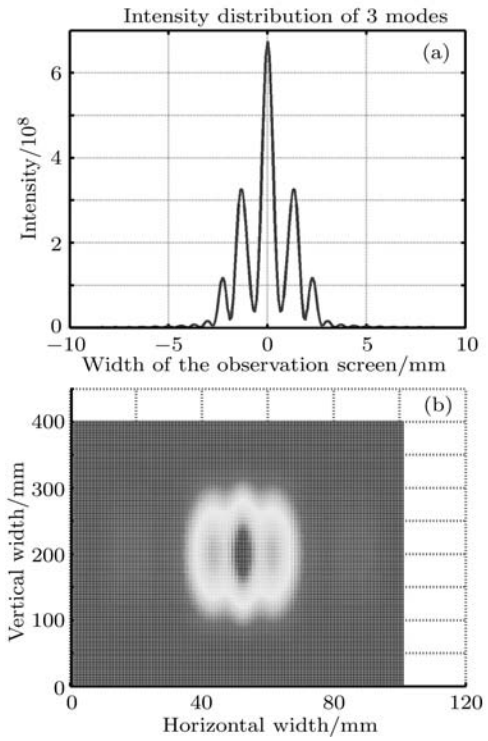


Fig. 3. Theoretical simulation results of three-mode oscillations, showing (a) the far field intensity distribution of the output beam and (b) the output beam cross section at 4.5 m.

Figure 3 shows the far-field intensity distribution and the cross section of the output beam when there are three oscillation modes in the cavity. In this situation, the optical field of the waveguide array is coupled into three groups which oscillate at one frequency separately. In Fig. 3(a), it can be seen that the far-field intensity distribution is a spatially suppressed distribution with three peaks and negligible side lobes; in Fig. 3(b), it is demonstrated that the cross section of the output beam at 4.5 m is three one-dimensional interference strips symmetrically distributed.

3. Experimental setup

The slice waveguide array laser structure used in this experiment is shown in Fig. 4. The total width of the slab gain region is 20 mm, and the height of the slab gain region is 2 mm. The aluminum top electrode is sliced into 10 parallel strips and each strip is 100 mm in length and 1.5 mm in width. The slit between two neighbouring strips is fixed at 0.4 mm in width and 2 mm in depth. By using this structure, a gain waveguide array is obtained; the laser optical field in each strip can be mixed with the laser optical field in its neighbouring strips over the narrow slits to achieve phase locking.

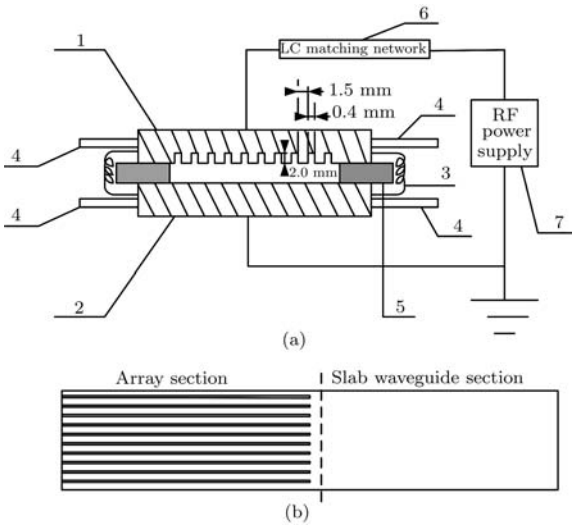


Fig. 4. Schematic diagram of the laser head structure, showing (a) the cross section of the laser head and (b) the vertical view of the top electrode. 1: Aluminum top electrode, 2: aluminum bottom electrode, 3: matching inductor, 4: water cooling tube, 5: ceramic insulating plate, 6: LC matching network, and 7: RF power supply.

The experimental setup is illustrated in Fig. 5, the laser output beam travels through a ZnSe beam splitter and is divided into two parts. The reflected part is reflected by a copper reflector again and directed into an infrared Burleigh CFT-500 scanning interferometer, and then received by a nitrogen cooled HgCdTe detector which detects and delivers the optical mode

scanning signal to the Tektronix TDS2012B digital oscilloscope. The transmission part travels through a ZnSe lens with a focal length of 127 mm and enters into a beam intensity distribution scanner located in the focal plane of the ZnSe lens. A LeCroy wavePro 7000 oscilloscope is connected to the beam scanner to show the far-field intensity distribution of the laser beam, meanwhile a reflector is set in front of the ZnSe lens to intercept and reflect the beam for the free propagation to the far field at a distance over 4 m without focusing when the burnt pattern is needed to be obtained.

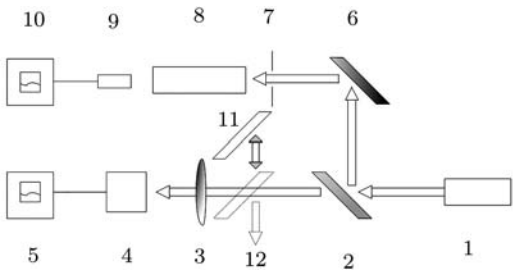


Fig. 5. Schematic diagram of the experimental setup arrangement. 1: Laser head, 2: ZnSe beam splitter, 3: ZnSe lens, 4: intensity distribution scanner, 5: LeCroy wavePro 7000 oscilloscope, 6: Copper reflector, 7: aperture, 8: CFT-500 interference scanner, 9: HgCdTe detector, 10: Tektronix TDS2012B digital oscilloscop, 11: Copper reflector, and 12: beam free propagation direction.

Tap water is used to cool the top and the bottom electrodes. An RF power supply at a frequency of 95 MHz is used to drive the gas discharge and the RF power is coupled into the discharge plasma through a low-pass matching network. The gas composition used is in a mixture of CO_2:Ne:He:Xe=1:1:3:0.5%. The optical resonator is a case-1 type optical waveguide resonator.[8] The output coupler of the resonator is a flat ZnSe mirror with a transmission of 10% and the feedback mirror of the resonator is an uncoated flat copper mirror with a reflectivity of 98%. The gas pressure is 8.55 kPa and the RF input power is 400 W with a reflected power less than 5%.

4. Experimental results

With the above experimental setup, the optical oscillation mode frequency, the far field intensity distribution and the corresponding output beam burnt pattern of the waveguide array laser are obtained.

Figure 6 shows the experimental results when there is only one mode oscillating in the waveguide array cavity. Figure 6(a) shows the optical field oscillation mode, figure 6(b) displays the burnt pattern of the output beam obtained at a free propagation distance of 4.5 m without focusing and figure 6(c) exhibits the far-field intensity distribution. From Fig. 6, it can be seen that when there is only one mode oscillating in the cavity, the far-field intensity distribution has a single peak without side lobes and the burnt pattern is a spatially suppressed single strip, which is a consequence of the spatial interference of multiple beams.

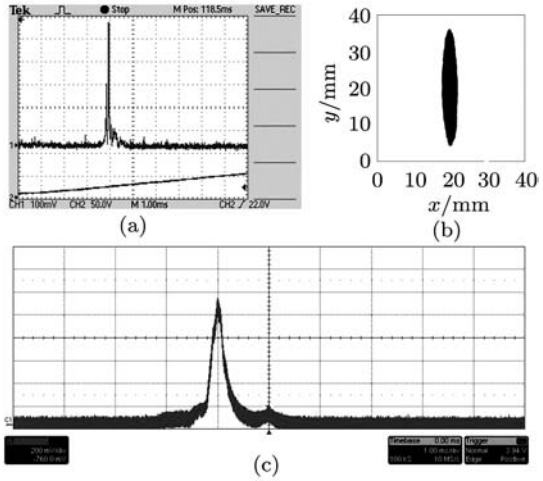


Fig. 6. Experimental results for one-mode oscillation, showing (a) oscillation mode, (b) output beam burnt pattern at 4.5 m, and (c) far field intensity distribution of the output beam.

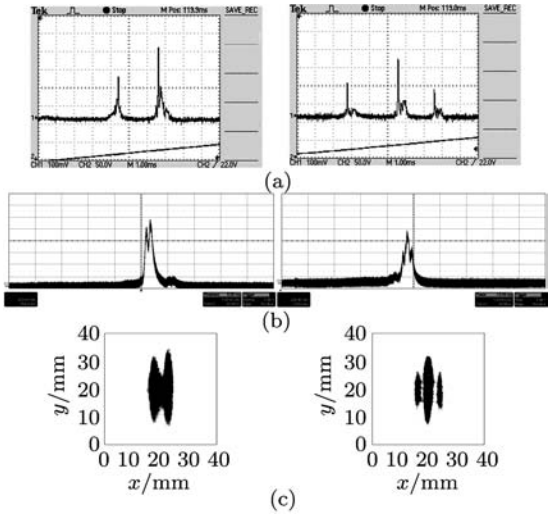


Fig. 7. Experimental results for two-mode (left) and three-mode oscillations (right), showing (a) oscillation modes, (b) far field intensity distribution of the output beam, and (c) output beam burnt pattern at 4.5 m.

Figures 7 shows the experimental results for two oscillation modes and three oscillation modes in the cavity. Figure 7(a) indicates the optical field oscillation mode, figure 7(b) displays the burnt pattern of the output beam at a free propagation distance of

4.5 m without focusing and figure 7(c) shows the far-field intensity distribution.

5. Discussion and conclusion

Comparing the above theoretical simulation results with the experimental results, it can be seen that the theoretical simulation results are in good agreement with the experimental results. In Fig. 1, when there is one oscillation mode, the far-field intensity distribution is a spatially suppressed single peak distribution with two negligible side lobes and the cross section of the output beam is a spatially suppressed single strip, which is in quite good agreement with the experimental results presented in Fig. 6. When there are two oscillation modes or three oscillation modes, the simulation results based on Eq. (7), as shown in Figs. 2 and 3, are in good agreement with the experimental results as shown in Fig. 7.

In conclusion, for the sliced waveguide array, we present a revised theoretical mode expression based on the Gaussian mode expression and the normal mode expression of the rectangle waveguide, which is an aperture Gaussian field distribution outside the waveguide. When the sliced waveguide array is in-phase locked, the field distribution can be expressed by the aperture Gaussian as

$$E(x) = \left\{\sum_{n=1}^{N} \sin\left(\frac{n\pi}{N+1}\right) \exp\left[-\frac{x_n^2}{w^2(z)}\right] \times \exp\left[-\mathrm{i}k\left(z+\frac{x_n^2}{2R(z)}\right)\right] \frac{1}{w(z)} \mathrm{rect}\left(\frac{x_n}{a}\right)\right\} \times \exp(\mathrm{i}\beta z).$$

In additin, the corresponding experimental work is carried out. The obtained results are in quite good agreement with the simulation results based on the presented revised theoretical mode expression.

References

[1] He X, Yang S, Harrison J, Feitisch A and Ovtchinnikov A 1999 *Electron. Lett.* **35** 1739

[2] Endriz J G, Vakili M and Browder G S 1992 *IEEE J. Quantum Electron.* **28** 952

[3] Menard S, Vampouille M, Colombeau B and Froehly C 1996 *Opt. Lett.* **21** 1996

[4] Goodno G D, Komine H and McNaught S J 2006 *Opt. Lett.* **31** 1247

[5] Xin J G, Zang E J and Wei G H 1994 *Opt. Eng.* **33** 1142

[6] Abramski K M, Baker H J, Colley A D and Hall D R 1992 *Appl. Phys. Lett.* **60** 2469

[7] Zhong Y H and Xin J G 2006 *Chin. J. Lasers* **33** 1030

[8] Sha P F, Xin J G, Fang L P, Liu Z F, Zhou Y, Zhang H L, Yu S L and Wen J G 2010 *Opt. Lett.* **35** 2329

[9] Wu X F, Yang J and Xin J G 2007 *Chin. Phys.* **16** 1031

[10] Tang X J, Zhao Z H and Xin J G 1999 *Acta Phys. Sin.* **48** 1236 (in Chinese)

[11] Butler J K, Ackley D E and Botez D 1984 *Appl. Phys. Lett.* **44** 293

[12] Hornby A M, Baker H J, Colley A D and Hall D R 1993 *Appl. Phys. Lett.* **63** 2591

[13] Katherine D L and William H S 1976 *Appl. Opt.* **15** 1334

[14] Abrams R L 1972 *IEEE. J. Quantum Electron.* **8** 838

[15] Henderson D M 1976 *Appl. Opt.* **15** 1066

[16] Ammon Yariv 2002 *Optical Electronics in Modern Communication* (Beijing: Electronics Industry Press) pp. 549–558

[17] Streifer W and Scifres D R 1986 *Appl. Phys. Lett.* **49** 1496